The Many Faces of Tunneling

E. J. Heller

Departments of Chemistry and Physics, Harvard University, Cambridge, Massachusetts 02138

Received: July 15, 1999; In Final Form: September 13, 1999

We consider classically forbidden events which control chemically and spectroscopically important processes. We focus on dynamical tunneling, which is tunneling in the absence of potential barriers, and tunneling between two Born−Oppenheimer potential energy surfaces. The former drives intramolecular vibrational relaxation (IVR) in molecules; the latter controls much of photochemistry, spectroscopy, and energy transfer.

I. Introduction

Semiclassical concepts and methods have been very useful in spectroscopy, where convenience and intuitive power are compelling reasons to use them.[1−3] One of the lessons of the semiclassical methods is that, very often, spectral features are due to essentially classical motion on potential energy surfaces, possibly with interference between alternate classical paths.

It is a truism that semiclassical concepts and methods frame the discussion of tunneling events too, although here one's ordinary classical intuition may not always be a reliable guide to what might happen. This paper focuses on novel tunneling events which sometimes tax our intuition and yet finally yield, very usefully, to a semiclassical analysis.

The concept of quantum tunneling, like chemical bonding, is almost second nature, and yet capable of surprising us with new facets. We recognize tunneling when we see it; invoke it when needed, and often presume to understand it. Yet, like chemical bonding, it has its subtleties, its difficulties. The subject still stirs interest and debate.

Why is the tunneling concept needed at all? What good is it really, when we all know that quantum mechanics is the correct theory and tunneling need not be discussed except in relation to a wrong (i.e., classical) description of the world. The danger of this view is illustrated by the difficulty of imagining say an $A + BC \rightarrow AB + C$ chemical reaction as a highly correlated wavefunction evolving simultaneously in six dimensions. We *can* however imagine a reaction mechanism involving a specific atomic choreography. The "divide and conquer" nature of classical mechanics, through the agent of the classical trajectory, allows us a powerful conceptualization and visualization tool. Moreover, the computer finds classical mechanics exceedingly easy to do, one trajectory at a time, in situations where quantum calculations are entirely out of the question for the foreseeable future. In order to use the classical visualization and the numerical trajectories we must know the relation of classical mechanics to quantum reality. One of the most important corrections to classical mechanics is tunneling; it is thus it is important to understand it.

In this paper we focus on two types of tunneling: (a) *dynamical tunneling*,[4−7] (as opposed to barrier tunneling) and (b) tunneling between two Born−Oppenheimer potential energy surfaces. Loosely, dynamical tunneling involves a quantum flow to places where classical dynamics does not go, when potential energy barriers are not to blame. Dynamical tunneling is more subtle than barrier tunneling because the barrier is not obvious from energy constraints.[37] For this reason dynamical tunneling often goes unnoticed or unappreciated.

Surface-to-surface Born−Oppenheimer tunneling involves getting from one adiabatic surface to another under circumstances where drastic changes in position or momentum are required of one or some linear combination of coordinates. There are many new effects and subtleties in this regime, some of which we hope to convey.

In special circumstances, extended (e.g., to complex time) classical mechanics can describe some tunneling events, such as barrier penetration in one dimension, or in more dimensions for separable motion. The Wentzel−Kramers−Brillouin (WKB) method for tunneling is a familiar example. However, the naked truth is that these methods are rather limited. For example, if the barrier is not very high, the WKB method is badly in error for all energies, both below and above the barrier! (Above the barrier we might want to compute the probability of reflection, another classically forbidden event.) The not-very-high barrier is a very common problem occurring in many dynamical tunneling situations. (These might be better termed "dynamical classically forbidden reflection", but dynamical tunneling is easier.) We shall discuss what to do in such situations below.

II. Dynamical Tunneling

A. Tunneling of an Asymmetric Top. A dramatic example involving tunneling of an asymmetric top (and more complicated cases involving rotation-vibration coupling) has been emphasized by Harter.[8] A symmetric top has the body fixed z-axis projection of the total angular momentum K as a constant of the motion. The eigenstates of nonvanishing K are doubly degenerate; $+K$ and $-K$ have the same energy. Introducing an asymmetry (so that the moments of inertia $I_1 \neq I_2 \neq I_3$) breaks this degeneracy. The splitting is typically quite small and can be extremely small for large angular momentum **J**. The spectrum of an asymmetric rigid rotor as a function of the asymmetry (Figure 1) reveals the splittings as they get larger toward maximum asymmetry ($I_2 = 0.4$ in this example).

Harter defines a "rotational energy" surface to lie at a radial distance from an origin $r = \gamma E(J'_x, J'_y, J'_z)$ proportional to the rotational energy $E(J'_x, J'_y, J'_z)$, depending on the body fixed components of angular momentum for a given $|\vec{J}|$, where γ is the proportionality constant. The rotational energy surface is illustrated in Figure 1 for $I_1 = 0.2$, $I_2 = 0.4$, and $I_3 = 0.6$. Classical dynamics proceeds along the contours on the RE surface, which are intersections of $E =$ fixed spheres with the $|\vec{J}| =$ constant RE surface.

10.1021/jp9924171 CCC: $18.00
Published on Web 11/20/1999

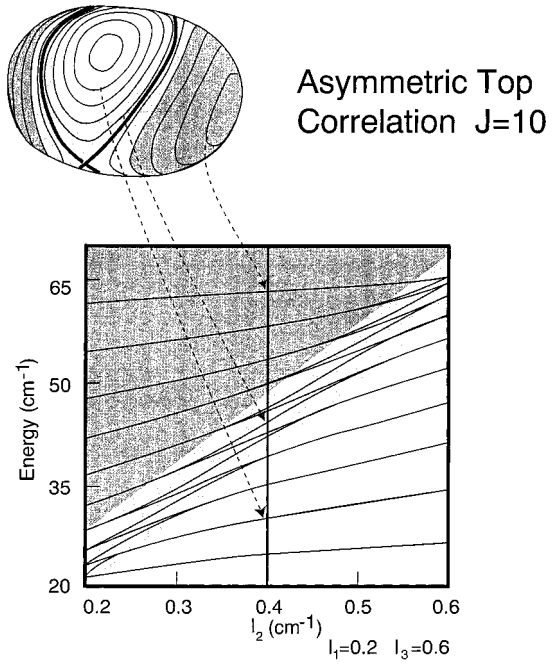

Figure 1. The rotational energy surface (above) and the energy correlation diagram as a function of asymmetry between prolate and oblate symmetric tops. Note the smallest splitting between the tunneling doublets occurs near the symmetric top limits and between states which correspond to distant level curves on the rotational energy (RE) surface. For example, states in the gray area tunnel across the separatrix rather easily, giving larger splittings.

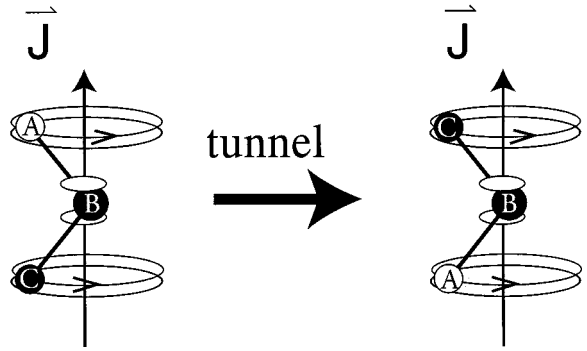

Figure 2. The bent ABC triatomic molecule shown here, treated as a rigid asymmetric top, can be initially put in a wave packet state of definite **J** with the atom A on top. Classically atom A remains on top forever, but quantum mechanically a tunneling takes place which switches A and C without changing **J**.

The bent ABC triatomic molecule shown in Figure 2, treated as a rigid asymmetric quantum top, can be initially put in a wavepacket state of definite **J** with the atom A above, as illustrated. This corresponds to rotation about the low moment of inertia body fixed axis. Classically, atom A remains above forever, but quantum mechanically a tunneling takes place which switches A and C without changing **J**. C appears up on top alternately with A, with a period given by the splitting. This corresponds to tunneling to the equivalent rotational energy contour on the backside of the RE surface (there are three reflection planes through the middle of the figure). Harter demonstrates that the tunneling splitting can often be accurately determined by a WKB tunnel integral, keeping $|\vec{J}|$ fixed.

This is the first but not the last encounter we shall have with tunneling across a separatrix. The separatrix is here defined by the pure unstable axis motion of an asymmetric top, and its characteristic hyperbolic zone is visible in Figure 1.

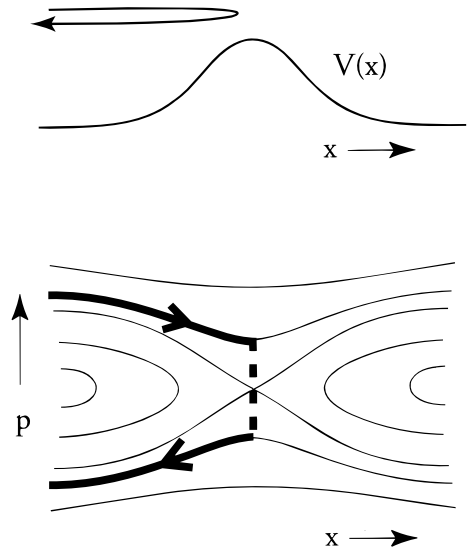

Figure 3. Phase space diagram illustrating the classically forbidden "dynamical tunneling" corresponding to reflection above a barrier.

B. Above-Barrier Reflection. Our second encounter with a separatrix is a little different. The seemingly simple problem of reflection above a barrier generates a separatrix in phase space and provides a powerful paradigm for dynamical tunneling. We review the case of a large barrier first, and then consider what happens for a small barrier. This discussion follows that in ref 9.

1. Large Barrier. Consider the reflection coefficient of a particle of energy E incident from the left on an potential barrier. The usual semiclassical reflection coefficient is

$$R = \exp(-2/\hbar\, I \int_{-p_o}^{p_o} x(p')\mathrm{d}p') \tag{1}$$

where p_o is the classical value for momentum at the center of the potential, $x(p)$ is the classical solution for the position in terms of momentum, and I stands for the imaginary part. The barrier penetration formula is more familiar, which is of the form eq 1 with the exchange of the roles of position and momentum: the barrier tunneling probability at energy E is

$$\mathrm{T} = \exp(-2/\hbar\, I \int_{-x_o}^{x_o} p(x')\mathrm{d}x') \tag{2}$$

where $\pm x_o$ are the classical turning points and $p(x) = \sqrt{2m(E-V(x))}$; m is the mass and $V(x)$ is the potential energy (see also Figure 3).

2. Small Barrier. It is well-known that the WKB formulas break down for energies near the top of the barrier. It follows that they fail catastrophically everywhere if the barrier is too small.

Fortunately, we can use perturbation theory if the bump is small. In the Born approximation, we start with a plane wave basis representing free particle motion; the effect of the potential is to induce transitions between right and left traveling plane waves: $E = \mathrm{e}^{\pm i/\hbar px}$ where $p = \sqrt{2mE}$. Choosing states normalized to unit flux, we obtain the reflection coefficient

$$\mathrm{R} = \frac{m^2}{\hbar^2 p^2}\left|\int_{-\infty}^{\infty} V(x)\mathrm{e}^{2i/\hbar px}\,\mathrm{d}x\right|^2 \tag{3}$$

which is the Born scattering result.[10] This formula is valid under certain "smallness" conditions of the potential: we need

$$\left|\frac{V(x)a}{\hbar v}\right| \ll 1 \tag{4}$$

where $v = p\hbar/m$ is the classical velocity of the particle and a is the width of the potential, which essentially requires the scattering potential to be weak compared to the kinetic energy of the incoming particle.[10]

3. A Semiclassical Distorted Wave Born Approximation. It can easily happen that the potential barrier is too high to be treated perturbatively, yet the action $\int^p x(p')dp'$ is too small compared to $\hbar$ for semiclassics to be reasonably applied. For such stronger potentials, WKB wave functions may play the role of the distorted wave basis: they are *exact* solutions to a well behaved, Hermitian Hamiltonian H_{WKB},[9] and we need merely take the difference potential $H - H_{WKB}$ as a perturbation. The WKB wavefunctions for a potential $V(x)$ may be written as linear combinations of wavefunctions of the form

$$\psi^{\pm}_{WKB}(x) = \frac{1}{\sqrt{p(x)}}\exp(\pm i/\hbar \int^x p(x')dx') \tag{5}$$

where $+(-)$ represents the right-(left-)going wave. As they satisfy Schrödinger's equation to first order in $\hbar$, we may expect that any "quantum" behavior shows up $O(\hbar^2)$ (or higher). Indeed it is easily demonstrated that

$$\left(-\frac{\hbar^2}{2m}\frac{d^2}{dx^2} + V(x) - E\right)\psi^{\pm}_{WKB}(x) = \hbar^2\left(\frac{-3p'(x)^2}{8mp(x)^2} + \frac{p''(x)}{4mp(x)}\right)\psi^{\pm}_{WKB}(x) \tag{6}$$

Writing the momentum derivatives in terms of potential derivatives and defining an effective potential for the WKB states as (primes represent derivatives with respect to x here)

$$V_{eff}(x, E) = V(x) - \hbar^2\left[\frac{5}{32m}\left(\frac{V'(x)}{E - V(x)}\right)^2 + \frac{V''(x)}{8m(E - V(x))}\right] \equiv V(x) - V_{tun} \tag{7}$$

we have

$$\left(-\frac{\hbar^2}{2m}\frac{d^2}{dx^2} + V_{eff}(x, E) - E\right)\psi^{\pm}_{WKB}(x) \equiv (H_{WKB} - E)\psi^{\pm}_{WKB} = 0 \tag{8}$$

Thus the WKB wavefunction exactly solves a quantum mechanical Hamiltonian problem with real potential which is smooth for energies above any potential maximum. We may think of the difference between the effective and exact potentials $V_{tun}(x, E) = V_{eff}(x, E) - V(x)$ as a perturbation which "turns off" quantum reflection. Schematically, we write

$$H = H_{WKB} + V_{tun} \tag{9}$$

where V_{tun} is of order $\hbar^2$ and induces the correct tunneling, and where H_{WKB} is "quantum mechanics without the tunneling". The dream of such a separation is realized here in this special example, and although we do not know how to make this separation work smoothly in general, it is a paradigm of a very important problem: dynamical tunneling.

The distorted wave Born approximation for the perturbation $-V_{tun} = V - V_{eff}$ between the ψ^+ and ψ^- is

$$R = \frac{m^2}{\hbar^2}\left|\int_{-\infty}^{\infty}(V(x) - V_{eff}(x))\frac{\exp(2i/\hbar\int^x p(x')dx')dx}{p(x)}\right|^2 \tag{10}$$

In ref 9, numerical trials showed that as we increase the size of the bump there is a gap in which the Born approximation for R is unsatisfactory and WKB has yet to become accurate. However, the WKB-distorted wave Born approximation works extremely well in this region. The lesson to be taken here is that if we can construct the primitive WKB solution, which does not "know" about above barrier reflection, we can obtain the reflection accurately by perturbation theory. Above barrier reflection is certainly a type of dynamical tunneling: the flow of quantum amplitude into classical forbidden domains where there is no potential energy barrier.[11] Above barrier reflection is also essentially diffraction, although that term is sometimes applied to classically allowed processes.

A classical phase space picture, Figure 3, illustrates contours for a barrier. The quantum reflection process is indicated by the dashed line from the top curve to the bottom. The Born approximation uses states attached to the p = constant lines, and the distorted wave Born approximation uses the distorted E = constant basis.

4. Numerical Results. In Figure 4 we present the results of the WKB−Born result, with the exact quantum reflection coefficient (see ref 10 for example), the semiclassical result, and the Born result (where applicable) for a sech^2 barrier $V(x) = V_o\mathrm{sech}^2(\alpha x)$.

C. More about Barriers. One would think that everything about tunneling and reflection in one dimension was familiar by now. However, it was not until very recently that an old controversy was resolved concerning the relationship of above-barrier classical trajectories and below-barrier tunneling.[12]

The seemingly reasonable argument that above-barrier trajectories contain the information about tunneling goes as follows. Consider a barrier peaking at $x = 0$, and construct the semiclassical time Green's function $G^{sc}(x, x', t)$ where x and x' straddle the barrier. There is always one trajectory going from x to x' in time t: at short times, a nearly free particle with high energy clearly suffices, and at longer times any time delay necessary is possible by "hanging up" near the barrier top with energy just above-barrier. Thus $G^{sc}(x, x', t)$ is well defined. Now we Fourier transform $G^{sc}(x, x', t)$ into the energy domain, choosing an E below the barrier:

$$G^{?}(x, x', E) = \int e^{-iEt/\hbar} G^{sc}(x, x', t)\, dt \tag{11}$$

where the question mark indicates the choice to do the integral exactly or by stationary phase. If the latter, then no stationary phase point is found for real time, and one must be sought in the complex time domain.[13] The search is successful and leads to the usual WKB under-the-barrier complex tunneling path.

Remembering that stationary phase is approximate, why not just do the integral in eq 11 exactly? Then we should get a better result, and furthermore the input to the integrand comes entirely from trajectories going under the barrier. In support of this idea, we note it is exact for an inverted harmonic oscillator barrier, where the semiclassical $G^{sc}(x, x', t)$ is exact and exact Fourier transform must give the correct result.

However, the idea is wrong in principle! We can schematically indicate the problem from an analytical-complex plane viewpoint and from a phase space viewpoint. Figure 5 shows the real time path (path A) of an integral in the complex time plane. This we suppose represents the integration path in eq 11. In search of a stationary phase (saddle) point, we distort

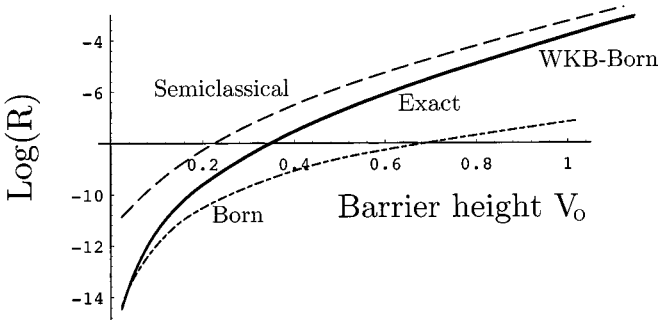

Figure 4. Comparison of WKB, Born, and WKB−Born approximations for reflection above a barrier as a function of barrier height V_o for the potential $V(x) = V_o\ \mathrm{sech}^2(x)$ for $E = 1.9$ and $H = p^2/2 + V(x)$. The exact and WKB-Born results are indistinguishable over this range.

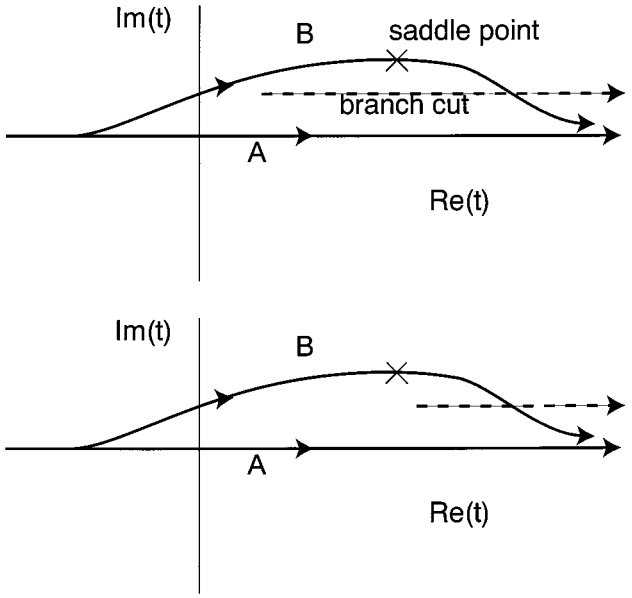

Figure 5. (Top) Integration paths for the stationary phase evaluation of the tunneling integral (path B) and the original integral (path A). Path B ends up on a different sheet of the integrand, and is not the original integral. (Bottom) As the points x and x' approach the barrier, in effect the saddle point comes out from the shadow of the branch cut and the two paths give similar answers. The path going above the branch cut is on the second physical sheet and corresponds to a different position of the trajectory.

the time contour above a branch cut in the complex plane, path B. Picking up the saddle point and then returning to the real time axis *on the upper sheet* gets the trajectory to tunnel under the barrier. Now comes the crucial point: the integral we just did by stationary phase is not the original integral! For example it wound up on a different sheet of the branch cut. *If we want to do an integral better than stationary phase, we should do path B numerically, not path A.* If we do this, the input trajectories are under-the-barrier ones, and so from this viewpoint we have seen it is not the over the barrier trajectories which are responsible for tunneling.

Some further comments are in order. First, in the case of an inverted harmonic oscillator, there is no branch cut, and so our argument does not apply, allowing the over-the-barrier interpretation. However we should note that the inverted oscillator is unphysical at large distance from the barrier top. The branch cut results from the potential flattening out at long range. A second comment concerns another aspect that can mislead or lull one into a false (but perhaps a useful!) sense of security.[14] If x and x' are close to the barrier, then (again schematically)

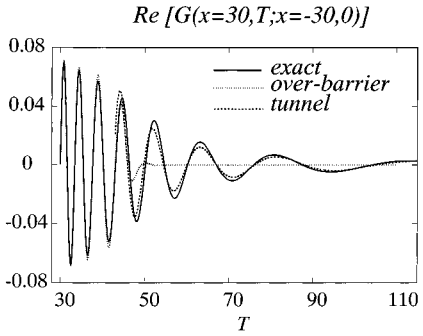

Figure 6. The above-barrier only, above-barrier + below-barrier, and exact Green's function propagator for the sech^2 potential barrier, from ref 12.

the saddle point starts to approach the branch point and the values of the two integrals, paths A and B, are not so different. This actually leads to a practical procedure, useful if x and x' are close in.[14] However as x and x' recede, the integral along path A goes to 0.

It was demonstrated in ref 12 that if one includes tunneling trajectories in the time domain, that is, if $G^{sc}(x, x', t)$ is augmented by under-the-barrier trajectories, then numerical Fourier transform of $G^{sc}(x, x', t)$ does work. It was shown that such classically forbidden, under-the-barrier trajectories actually make a larger contribution than the over-the-barrier, classically allowed ones at long times. The under-the-barrier trajectories give a contribution which is exponentially small but with weak time dependence; the over-the-barrier trajectories are exponentially depleted at long times and have a strong (exponentially damped) time dependence. Figure 6 gives the relative contributions for a typical $\mathrm{sech}^2(x)$ potential barrier. The dominance of a classically forbidden process over a classically allowed one cannot survive the theorist's limit $\hbar \to 0$, since the tunneling process will typically scale as $\exp(-c/\hbar)$, where c is a constant, but experiments are done at finite $\hbar$!

D. The Photoelectric Effect, Photoionization, etc. Having treated what we claim is the paradigm of dynamical tunneling, i.e., reflection above a barrier, we now turn to some physical situations where it arises.

Consider a Morse oscillator initially in its ground state. Suppose we apply weak monochromatic radiation, which is resonant (in the quantum sense) with a high lying bound state with $h\nu \gg \hbar\omega$, where ω is the local frequency of the oscillator near its minimum and ν is the frequency of the radiation. This process is classically forbidden: the frequency of the perturbation is much too high to pump much energy in or out of the oscillator. Essentially nothing happens classically, while quantum mechanically we know a certain fraction of the amplitude will be promoted to the excited state. The classically nonresonant absorption is a classically forbidden process, and a fine example of dynamical tunneling. This discussion applies to any nonresonant single-photon process, such as photoionization of Helium or the photoelectric effect. Indeed, the usual textbook discussion of the photoelectric effect, an example of the need for quantum mechanics, is a statement that the photoemission process fails classically under the circumstances of the experiment (weak, classically nonresonant light), yet is allowed quantum mechanically.

It is interesting to assign a harmonic oscillator of angular frequency $2\pi\nu$ to the field, as in quantum electrodynamics, and treat it as a degree of freedom coupled to the Morse potential. Suppose there are four quanta in the field mode, and zero in the oscillator initially. This state is by design almost degenerate

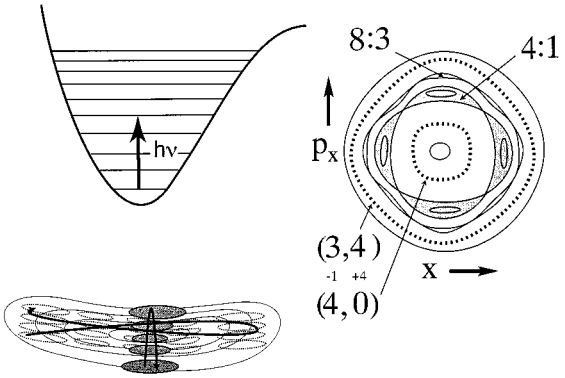

Figure 7. (Top left) The usual energy representation of a one-photon, multiquantum transition. (Bottom left) A coordinate space picture, illustrating the potential, the wavefunctions of the field oscillator, the Morse oscillator, and arrows indicating the qualitative classical motion corresponding to the initial and final states. (Right) Poincare' surface of section for the field oscillator-Morse oscillator problem, showing resonance zones in phase space corresponding to the 4:1 resonance. However, even in the presence of the resonance and the coupling, the initial torus representing energy mostly in the field oscillator is almost undistorted from what it would be without the coupling to the field. Motion is confined to the invariant surfaces seen here, corresponding to the classical "no-go" for the transition.

with three quanta in the field and four in the oscillator. Although this implies the existence of a 4:1 resonance in the classical phase space (see below), the resonance will generally not directly affect a trajectory representing the initial oscillator and in any case will be so narrow (for weak coupling) that it barely excites the oscillator. The usual energy diagram, as in Figure 7, top left, can be augmented in two ways, in coordinate space Figure 7, bottom left, and in phase space, Figure 7, right.

In Figure 7, bottom left, we sketch a schematic two dimensional oscillator potential illustrating the low frequency mostly *x*-direction (horizontal) motion of the Morse potential and the much tighter high frequency *y*-motion of the field oscillator. Eigenstates corresponding to the initial and final state as described above are sketched as well. These two motions do not communicate classically, but quantum mechanically there is a nonvanishing matrix element connecting them.

Figure 7, right, displays the phase space view of this, with the convention that a $y = 0$ (field oscillator) surface of section is constructed, in which x and p_x are plotted every time the trajectory penetrates $y = 0$ with $p_y > 0$. Resonance islands appear corresponding to the 4:1 resonance and higher order resonances. Now we can understand the relevance of the above-barrier reflection problem to dynamical tunneling: the local phase space structure near the islands is the same as the above-barrier problem[7,15−18] (see Figure 8). This means that we can use perturbation theory or distorted wave perturbation theory to determine the tunneling interaction between nearly degenerate states with different actions, in this case (4,0) and (3,4), just as we did for the barrier reflection problem.

E. Collisional Dynamical Tunneling. Many years ago Miller[19] noted that classically forbidden events appear in semiclassical scattering theory ("classical S-matrix theory") as action changes of the target which fail to reach a full quantum jump (action change of h or greater), for all initial conditions. Then, the "primitive" semiclassical cross section will be zero. However Miller also gave uniform expressions which correctly bootstrap the finite quantum transition amplitude from the failed classical attempt. (This same failure would become classically allowed if $\hbar$ were allowed to become much smaller). This is one of the first clear examples of dynamical tunneling-something

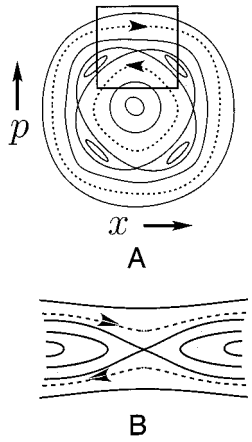

Figure 8. A Poincaré surface of section for a typical system with narrow resonance islands (A) and for a localized barrier (B). The local structure (see boxed region in A) is the same.

that happens quantum mechanically but fails to happen classically, but with no potential barrier to blame.

A related example involves vibrational relaxation in neat O_2, as studied for example by Faltermeir et al.[20,21] A classical study of the relaxation rate gives 0.0005 s^{-1}, many orders of magnitude slower than the experimental rate of 360 s^{-1}. For all practical purposes, the vibrational relaxation of an excited O_2 molecule in cold, liquid O_2 is classically forbidden, yet it proceeds slowly quantum mechanically. Under the conditions of the experiment, the vibrational frequency of the O_2 is $\omega_{vib} = 1552$ cm^{-1}; however, typical environment frequencies are a very off-resonant 50 cm^{-1}. Dynamical tunneling is the agent of the relaxation of neat O_2.

III. Dynamical Tunneling and IVR

In a polyatomic system, before strong chaos sets in at higher energy, phase space is densely filled with small resonance zones. While a process known as Arno'ld diffusion can lead to classical transport in phase space in many dimensions, this diffusion is typically extremely slow. The situation is probably rather like the neat O_2 example just cited: classically the process is not forbidden but the tunneling is much, much faster. Indeed we explicitly proved this is the case in resolving the over-the-barrier tunneling controversy in section II.C. Just as in the problem of tunneling under a barrier when viewed in the time domain, we expect a quantum tunneling process to dominate a classically allowed one if $\hbar$ is not too small, i.e., tunneling will dominate Arno'ld diffusion.

Every point on a surface of section has the same classical energy. If it should happen that two tori cutting through this surface quantize in the Einstein−Brillouin−Keller (EBK) sense, i.e., with actions I given by

$$I_1 = \left(n_1 + \frac{1}{2}\right)h,\ I_2 = \left(n_2 + \frac{1}{2}\right)h$$

$$I_1' = \left(n_1' + \frac{1}{2}\right)h,\ I_2' = \left(n_2' + \frac{1}{2}\right)h \qquad (12)$$

and also

$$H(I_1, I_2) = H(I_1', I_2') \qquad (13)$$

then degeneracy of two eigenstates is predicted semiclassically. However, quantum mechanics will find a way to connect the two tori by tunneling. The true eigenstates will be mixtures of

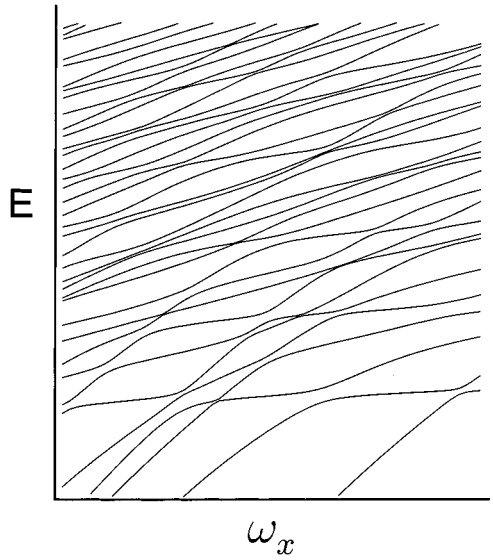

Figure 9. Avoided crossings as a function of a parameter. $H = p_x^2/2 + p_y^2/2 + \omega_x^2x^2/2 + \omega_y^2y^2/2 + 0.2xy + \lambda x^2y$, and the parameter ω_x was varied. The narrow avoided crossings are due to quantum tunneling; at low energies, the classical dynamics is integrable.

the two torus-localized states, which implies energy transfer (or phase space flow) which is not present classically. The tunneling will be accompanied by a splitting. A typical plot of energy versus a parameter for the first few eigenstates of a two dimensional anharmonic system is shown in Figure 9. This Hamiltonian is $H = p_x^2/2 + p_y^2/2 + \omega_x^2x^2/2 + \omega_y^2y^2/2 + 0.2xy + 0.2x^2y$, and the parameter ω_x was varied, near the region $\omega_y = 1.0$, $\omega_x = 1.0$, $\lambda = 0.1$. Isolated avoided crossings are clearly visible. Inspection of the eigenstates far from any crossing displays clean and easily countable nodal structure corresponding to classical motion with a given set of actions, but near an isolated avoided crossing the eigenstates become confused admixtures of two such states.[7]

A. Classical Resonance Analysis. We briefly outline the classical resonance analysis, which provides several avenues for dealing with the tunneling.

We can illustrate the situation starting with an integrable single resonance Hamiltonian for two degrees of freedom. Consider, following Ramachandran and Kay,[18]

$$H(\mathbf{I}, \boldsymbol{\theta}) = \omega_1 I_1 + \beta_1 I_1^2 + \omega_2 I_2 + \beta_2 I_2^2 + \lambda I_1 I_2\, \nu(\theta_1, \theta_2) \quad (14)$$

$$\equiv H_0 + V(I_1, I_2, \theta_1, \theta_2) \quad (15)$$

where $\nu(\theta_1, \theta_2)$ is periodic in the angle variables θ_i. The base frequency is given by thhe parameter ω_i and the diagonal anharmonicity is controlled by β_i. The potential terms $\nu(\theta_1, \theta_2)$ can usefully be expanded as

$$\nu(\theta_1, \theta_2) = \sum_{n_1,n_2}{}' \nu_{n_1,n_2}(n_1\theta_1 - n_2\theta_2) \quad (16)$$

where (n_1, n_2) are relatively prime numbers possessing no common factors (a prime over the summation sign reminds us of this). Then the functions $\nu_{n_1,n_2}(n_1\theta_1 - n_2\theta_2)$ contain all the $(n_1{:}n_2)$ resonance interaction and are expanded as

$$\nu_{n_1,n_2}(n_1\theta_1 - n_2\theta_2) = \sum_p \nu_{n_1,n_2}^{(p)} \exp[ip(n_1\theta_1 - n_2\theta_2)] \quad (17)$$

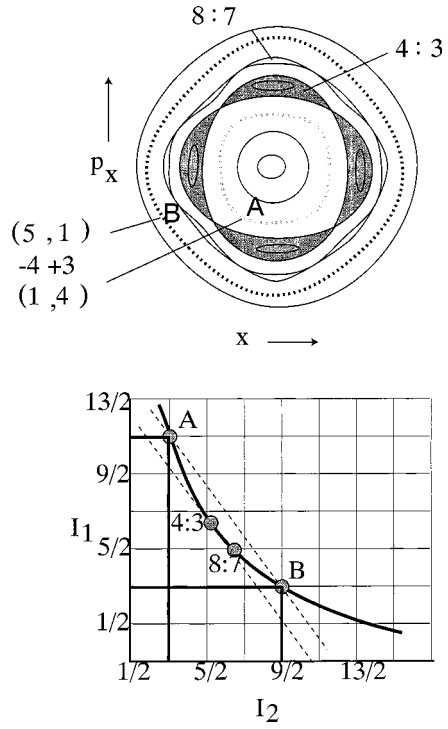

Figure 10. A 4:3 resonance mediates the tunneling between the $A = (^3/_2, ^{11}/_2)$ torus and the $B = (^9/_2, ^3/_2)$ torus. The solid heavy line shows the level curve of constant energy in action space; note that $E_A = E_B$. Somewhere in between points A and B will lie the actions where $\omega_1/\omega_2 = -(\partial H/\partial I_1)/(\partial H/\partial I_2) = -\partial I_2/\partial I_1|_E$; this is denoted by 4:3 and a black dot. At this point on the level curve, the tangent is parallel to the line drawn between *A* and *B*.

so that the potential has the expansion

$$\nu(\theta_1, \theta_2) = \sum_p \sum_{n_1,n_2}{}' \nu_{n_1,n_2}^{(p)} \exp[ip(n_1\theta_1 - n_2\theta_2)] \quad (18)$$

For example a 2:2 resonance zone would be induced by $\nu_{1:1}^{(\pm 2)}$.

Canonical transformation to new action-angle coordinates (J_1, J_2, ϕ_1, ϕ_2) is accomplished via the generator

$$F(\mathbf{J}, \boldsymbol{\theta}) = \frac{1}{2}J_1(\theta_1 - \theta_2) + \frac{1}{2}J_2(\theta_1 + \theta_2) \quad (19)$$

which gives

$$\phi_1 = \frac{1}{2}(\theta_1 - \theta_2);\ \phi_2 = \frac{1}{2}(\theta_1 + \theta_2) \quad (20)$$

$$J_1 = (I_1 - I_2);\ J_2 = (I_1 + I_2)$$

The Hamiltonian in the new coordinates is

$$H = \omega^- J_1 + \omega^+ J_2 + \beta^+ J_1^2 + \beta^+ J_2^2 + 2\beta^- J_1 J_2 + \frac{\lambda}{2}(J_2^2 - J_1^2)\nu_{1:1}^{(2)} \cos(4\phi_1) \quad (21)$$

$$\equiv H_0 + \frac{\lambda}{2}(J_2^2 - J_1^2)\nu_{1:1}^{(2)} \cos(4\phi_1)$$

where $\omega^{\pm} = (\omega_1 \pm \omega_2)/2$ and $\beta^{\pm} = (\beta_1 \pm \beta_2)$. It is clear that J_2 is a constant of the motion because ϕ_2 is absent in H. The phase portrait in the J_1, ϕ_1 plane for fixed energy E is shown in Figure 10, top. A single 2:2 resonance zone is seen. Now suppose the tori labeled *A* and *B* have exactly the same energy at the primitive (EBK) level; i.e., $H(I_1^A, I_2^A) = H(I_1^B, I_2^B)$ where I_1^A

$= (n_1^A + \alpha_1^A)h$, etc., where n_1^A is an integer and α_1^A arises from the well-known Maslov phase corrections. The heavy dashed lines to either side of the resonance zone are degenerate tori which are EBK quantized. Dynamical tunneling is expected between them. Even if the EBK energies differ, the states will be mixed if the tunneling interaction is larger or on the order of the EBK splitting.

We now demonstrate that the dynamical tunneling causing the avoided crossing is once again a case of an above-barrier reflection amenable to a perturbative treatment.

Suppose two states with quantum numbers (1,5) and (4,1) are involved in an avoided crossing. The resonance zone appears between the tori involved in the tunneling for the reason seen in Figure 10. A 4:3 resonance mediates the tunneling between the *A* torus with actions (1+1/2, 5+1/2) = (3/2,11/2) and the *B* torus with actions (9/2, 3/2). The heavy line delineates the level curve of constant energy in action space; note that $E_A = E_B$. By the mean value theorem, somewhere in between points *A* and *B* must lie actions where the slope *S* of the constant energy curve is equal to the slope of the line connecting the two sets of actions.

$$-S = \omega_1/\omega_2 = -\frac{\partial H/\partial I_1}{\partial H/\partial I_2} = -\left.\frac{\partial I_2}{\partial I_1}\right|_E \tag{22}$$

this is denoted by 4:3 and a black dot. At this point on the level curve, the tangent is parallel to the line drawn between A and B.

$S = -4/3$ corresponds to the zone in classical phase space where the resonance (4:3 in this example) exists. In this way we can always find an appropriate resonance zone which will connect two tori by over-the-barrier dynamical tunneling.

Even if the quantum numbers of the states involved in the avoided crossing are very different, say differing by *n* quanta in action I_1 and *m* quanta in I_2, there is in general an n:m classical resonance island chain lying between the tori corresponding to the states which is the agent of the quantum tunneling. In a generic coupled but nearly integrable phase space, an island chain will exist for every rational winding number. In this sense classical phase space structures are the cause even of very narrow avoided crossings between states of very different character.

B. Calculation of the Tunneling Interaction. There are several ways to calculate the tunneling between the tori caused by the intervening resonance zone. They all begin with a resonance analysis as just described. In two closely related approaches one gets the tunneling by stopping short of the fully semiclassical analysis, substituting a little quantum mechanics into the one dimensional effective Hamiltonian produced by the resonance analysis. This produces a "uniform" approximation; in essence one is doing full quantum mechanics on a classically pre-processed Hamiltonian. One approach quantizes the (J_1, ϕ_1) Hamiltonian for fixed J_2 with the Ansatz $J_1 \rightarrow -i\hbar \mathrm{d}/\mathrm{d}\phi_1 + \hbar$.[15,16] The resulting Schrödinger equation is then solved numerically, or analytically if possible. The pendulum-like Hamiltonian 21 contains the nonclassical below barrier tunneling (and above barrier reflection). A closely related scheme uses the Heisenberg (matrix) formulation of quantum mechanics by finding matrix elements of the resonant interaction term and diagonalizing. Bohr correspondence in invoked in the following way: the resonant term depends on both actions and angles of the nonresonant part of the Hamiltonian, as in eq 14. The actions appearing in the resonant term are set to their mean values ($\bar{J}_1$, $\bar{J}_2$) and the off-diagonal tunneling matrix element becomes

$$\langle J_1, J_2|H|J_1', J_2'\rangle \tag{23}$$

$$= \frac{1}{(2\pi)^2}\int\int \mathrm{e}^{ip(n_1\theta_1 - n_2\theta_2)} V(\bar{J}_1, \bar{J}_2, \theta_1, \theta_2)\, \mathrm{d}\theta_1\, \mathrm{d}\theta_2$$

$$\equiv V(\bar{J}_1, \bar{J}_2)^{(p)}_{n_1,n_2} \tag{24}$$

with $\bar{J}_1 = (J_1 + J_1')/2$, etc. The method is uniform since the matrix of EBK diagonal energies and off-diagonal couplings is numerically diagonalized. An example of the use of a procedure much like that just described is found in Roberts and Jaffe.[17]

C. Spectra and IVR Implications. It has been suggested that the weak tunneling interactions discussed here have profound effects on IVR and may even be one of the main agents of IVR.[7,22] The idea is that an unperturbed quantum state with zeroth order quantum numbers (I_1, I_2, ...,), adhering to a classical torus with those actions, is weakly coupled to a dense set of states with very similar energy and various actions. A study of the analytic properties of the matrix elements, eq 24, suggests it is reasonable to take the typical matrix element to scale as $V \sim \exp[-\gamma|\Delta I|]$ where *V* is the matrix element, γ is a proportionality factor, and ΔI is the total change of action in going form one state to another.

Suppose we start in the initial state with quantum numbers

$$(P, 0, 0. \cdots, 0) \tag{25}$$

where there are *L* modes listed. Suppose the first, occupied mode with *P* quanta in it has a frequency "typical" of the other modes, which have a narrow spread of frequencies. Then it generates a set of tiers which differ in the number of quanta removed from the first mode and distributed around the others, where the total number of quanta is constant.

The density of states with *Q* quanta distributed among (*L* − 1) modes varying over some finite range of frequencies with small anharmonicity goes as

$$\rho_Q = \frac{\exp[\mu Q]}{\sqrt{Q}} \tag{26}$$

This grows almost geometrically, so there will be a competition in the rate expression between the exponential decrease of the matrix elements and the exponential increase in the density of states, as tiers with greater action differences are considered. The outcome of the competition determines whether or not states are globally mixed into a sea of quasidegenerate states. If so, the character of the the initial state will fractionate into a quasidegenerate range of states whose width is given by the initial Golden Rule decay time. Measures have been developed which gauge the degree of mixing of unperturbed states into the eligible eigenstates.[27] The result of such fractionation has been seen experimentally and may be evidence for the tunneling mechanism given here. The effect on the spectrum of the tunneling interaction is shown schematically Figure 11; this kind of spectrum, with a 0.1 to 0.01 cm^{-1} bandwidth, has been seen in several medium sized molecules (such as propyne) at moderate energy (a few thousand wavenumbers).[24−26]

IV. Tunneling between Born−Oppenheimer Surfaces

So far we have concentrated on forbidden processes which, when properly analyzed, reduce to tunneling across a separatrix. We move now to a different situation, one involving an even more common circumstance in chemical physics: hopping between potential energy surfaces.

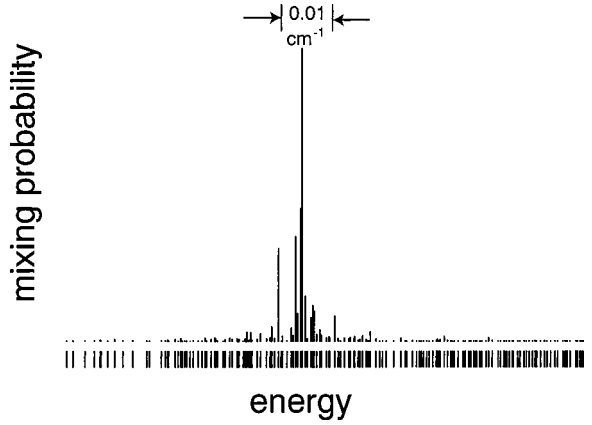

Figure 11. A fractionated spectrum of a zeroth-order state which, without the tunneling, would have been a single peak. The energies of the eigenstates are given as tic marks.

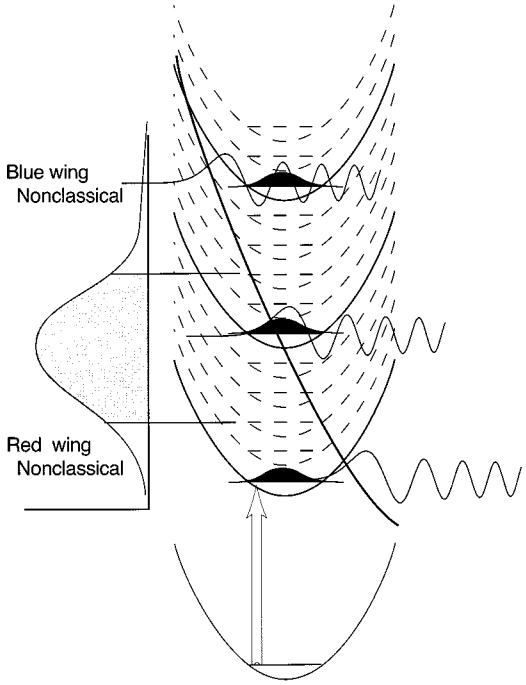

Figure 12. If the frequency of the radiation is too high or too low, the surface raised by $\hbar\omega$ fails to intersect the second surface in the classically allowed region, leading to a tunneling process requiring a position or momentum jump, and corresponding to the weaker "tails" or wings of the absorption spectrum.

A. Radiative Example: Classical and Tunneling Regimes. Both radiative and radiationless transitions depend on the overlap of vibrational states coupled by a weak perturbation. In the radiative case this coupling is the transition moment which is a function of the nuclear coordinates (after integrating over the electronic coordinates). In the radiationless case, the coupling is due to the nonadiabatic terms in the Hamiltonian, which again are functions of the nuclear coordinates. Given these similarities, it is useful to raise (lower) the initial Born−Oppenheimer surface by $\hbar\omega$ where ω is the frequency of the absorbed (emitted) light, and treat the radiative process much like a radiationless one.

Consider the absorption spectrum for a bound state going to a steep part of an excited electronic state as shown in Figure 12. As the incident light frequency is increased, we proceed from the "red" wing, through the band center, to the "blue" wing. Drawing a horizontal line between the two classical turning points of the "donor" or initial surface defines the classically allowed region of the donor wavefunction. At first the intersection of the surfaces occurs to the right of the classically allowed region, then within it, and finally to the left of it as ω is increased. Representative diagrams of the overlap of the two vibrational states are given in each of the three regions. When the surfaces cross in the classically allowed region, the overlap is good and the spectrum is near its maximum. When they cross outside the classically allowed region, the overlap is poor and corresponds to the nonclassical wings. This distinction extends to any number of dimensions, and defines the concept of the "nonclassical" region of Franck-Condon factors.

The issue is identical for radiationless transitions, except that one cannot lift the potential energy surfaces relative to each other (except for very small adjustments with external fields). Thus, the radiationless transition case is "stuck" at one value of the vertical displacement. Quite often, this value places the system in question in the nonclassical regime (as is the case for benzene during an electronic transition from the S_1 surface to the lowest singlet T_1 surface), and once again from there to S_0.

Nonclassical Franck−Condon factors are necessarily small, since either the amplitudes or the nodal structures (or both) of the two wave functions are incompatible. In the red wing, only the tails of the wavefunctions overlap; the integral is clearly small. This is shown in Figure 12, bottom. In the classical region, the amplitudes and nodes are compatible, and the overlap is large. In the blue wing, the nodes in one of the eigenstates kill the overlap even though the amplitude is fairly large for both states over a portion of coordinate space (Figure 12, top).

However, there is a subtle point about the blue wing Franck-Condon factors. There are two possibilities for interpreting their residual value. Either the residual results from an incomplete nodal cancelation in the region of large amplitude or it could come from the overlapping region of the tails of the two states, which after all still contribute. While this distinction may seem academic, we shall see that it leads to important effects in two or more dimensions.

B. Semiclassical Franck−Condon Factors. A traditional perspective on Franck−Condon factors is suggestive about tunneling between potential energy surfaces. Semiclassical eigenstates may be represented as a sum of terms of the form

$$\psi(x) \approx \frac{1}{|p(x)|^{1/2}}\exp(i\int p(x')\mathrm{d}x' + i\nu) \tag{27}$$

A Franck−Condon overlap between two such states, each on its own Born−Oppenheimer potential energy surface, is

$$\langle\psi_A|\psi_D\rangle \sim \int \frac{1}{|p_A(x)|^{1/2}|p_D(x)|^{1/2}} \exp(-i\int^x p_A(x')\mathrm{d}x' + i\int^x p_D(x')\mathrm{d}x')\,\mathrm{d}x \tag{28}$$

The stationary phase evaluation of this integral requires

$$\frac{\mathrm{d}}{\mathrm{d}x}(-\int^x p_A(x')\,\mathrm{d}x' + \int^x p_D(x')\,\mathrm{d}x') = 0 \tag{29}$$

or

$$p_A(x) = p_D(x) \tag{30}$$

which implies, since the total energy is the same on both potential energy surfaces,

$$V_A(x) = V_D(x) \tag{31}$$

This is the well-known result that the semiclassical contribution arises where potential energy surfaces cross. There may of course be more than one stationary phase point; in what follows, we shall assume we are dealing with the dominant contribution.

There are two possibilities for a crossing in the nonclassical regime. If it occurs at a real value of $x^\dagger$, then the position of the crossing is real and the momentum at the crossing, $p_A(x^\dagger) = p_D(x^\dagger)$ is pure imaginary. (Real momentum and real position correspond to the classical regime where no "jumping" is required). This is the case of a position jump, where the contribution to the integral is coming from the tails of the wavefunctions. Both $p_A(x^\dagger)$ and $p_A(x^\dagger)^*$ are stationary phase points, but one of them corresponds to exponentially increasing wavefunction and is discarded.

The crossing may however be at complex values of x. The momentum will no longer be purely imaginary, but will generally be complex. It often happens that the position is *mostly* imaginary, and the corresponding momentum is mostly real, giving a jump which is largely in momentum. If the crossing happens at $p = p^\dagger$, it also must occur for opposite sign $p = -p^\dagger$. For pure imaginary momentum this is the same as $p^{\dagger *}$, but generally there are four stationary phase momenta. Two give rise to increasing rather than decreasing wave functions in the classically forbidden region and are discarded, leaving two remaining. There may be constructive or destructive interference between these distinct but equal magnitude stationary phase amplitudes,[6,32] and if the resulting oscillations are seen it is a sign that momentum tunneling is taking place.

These considerations apply even if the initial state is the ground state, which is seemingly a dubious candidate for semiclassical approximation. However, we are using the semiclassical form usually deeply within classically forbidden region. As pointed out long ago by Miller,[13] semiclassical approximations should work well so long as the absolute value of the momentum is large enough. At a more exact level, we note the work of Nikitin[31] which builds on the work of Landau and Lifschitz,[10] demonstrating how semiclassical matrix elements involving even the ground vibrational state may be quite accurate.

The stationary phase evaluation of eq 28 also yields a prefactor. Since $p_A(x^\dagger) = p_D(x^\dagger)$, and

$$\frac{\partial^2 \int^x p(x')\,dx'}{\partial x^2} = \frac{\partial p(x)}{\partial x} \sim F(x)/p(x)$$

we have

$$\langle \psi_A | \psi_D \rangle \sim \sum \frac{1}{p(x)} \frac{p(x)^{1/2}}{|\Delta F|^{1/2}} \tag{32}$$

where ΔF is the difference in force experienced on the two surfaces at the crossing point, and the sum is over stationary phase points. The square of this is

$$P \sim \frac{2\pi\epsilon m}{\hbar p_\perp |\Delta F|} \tag{33}$$

where we have included a factor of ϵ to cover the overall electronic prefactor to the overlap integral. This is the Landau−Zener formula, here written using $p_\perp$, which is the momentum component perpendicular to the surface crossing in more than one dimension.

This formula is proportional to the area of intersection (black) of the two phase space curves, or alternately to the van Vleck determinantal prefactor for the stationary phase version of the integral (Figure 13).[28]

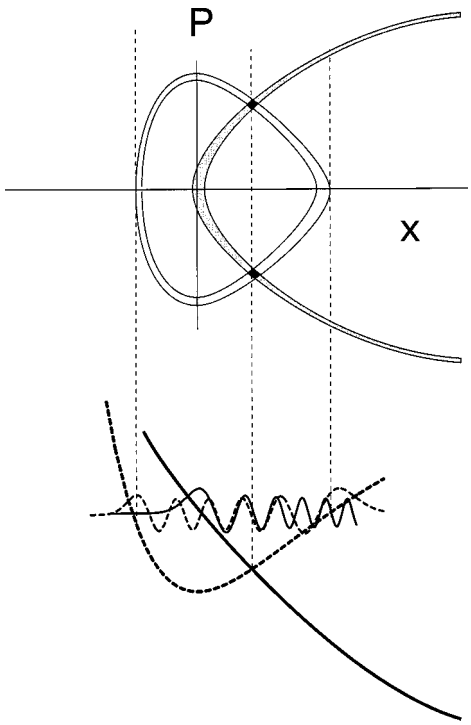

Figure 13. Phase space and coordinate space views of a Franck−Condon factor for two vibrational levels given by two Born−Oppenheimer potential energy surfaces crossing in the classically allowed region. In the black shaded regions of overlap in phase space the system may jump the track, so to speak, without change of position or momentum. Note the coordinate space region where both functions oscillate at the same rate; this is a region of stationary phase of the integral for the Franck−Condon factor, and coincides with the coordinate space location of the crossing in phase space.

C. Franck−Condon Factors for Forbidden Processes. We are interested primarily in the classically forbidden situation, where the Born−Oppenheimer surfaces do not cross in the classically allowed region, or when they do not cross at all, for real values of the coordinates. An enormous range of phenomena may be cast as tunneling between adiabatic potential energy surfaces. To name a few: slow radiationless transitions, photoabsorption in the wings of a band, predissociation of van der Waals molecules, slow charge transfer, and slow excitation transfer.

In Figure 14 we see a system which must tunnel, portrayed in coordinate and in phase space. From the phase space picture it is irresistible to suppose that in some sense the wavefunction the upper bounded potential curve (the inner curve in phase space) wants to jump to the other phase space track by hopping partly in position and partly in momentum along the path shown (arrows); this point of view was strongly reinforced in ref 29. For other points of view see also refs 10, 30−32.

The fascination with the tunneling case hinges on the strange possible outcomes of the the radiative or radiationless transition which the Franck−Condon factors describe. The really interesting cases involve deep tunneling in several degrees of freedom. Such events are commonplace in photochemistry, and much more could be done along these lines experimentally using control available in photoabsorption.

We develop a picture which is much simpler to visualize than the complex root solutions of eqs 30 and 31.[29,33,34] Consider the Golden Rule expression for the rate of the electronic transition,

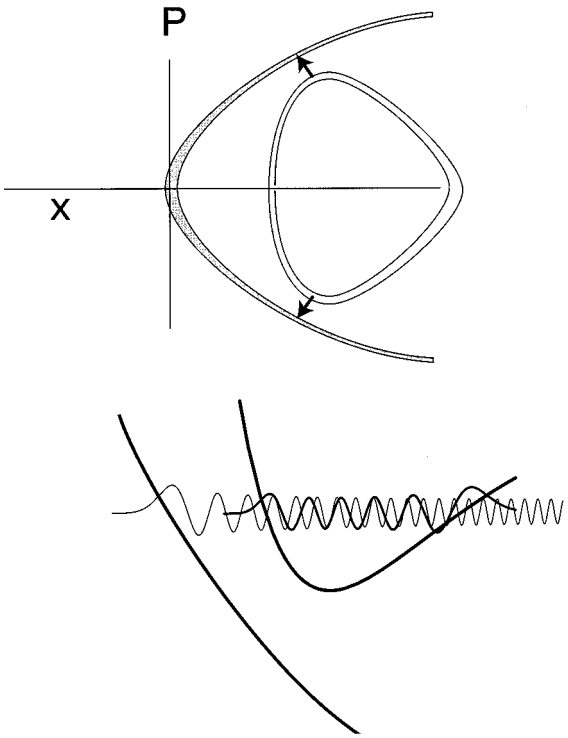

Figure 14. Phase space and coordinate space views of a Franck−Condon factor for two vibrational levels given by two Born−Oppenheimer potential energy surfaces crossing in the classically forbidden region. Nowhere do the wave functions on the respective surface oscillate alike, nor is there a stationary phase point for real coordinates.

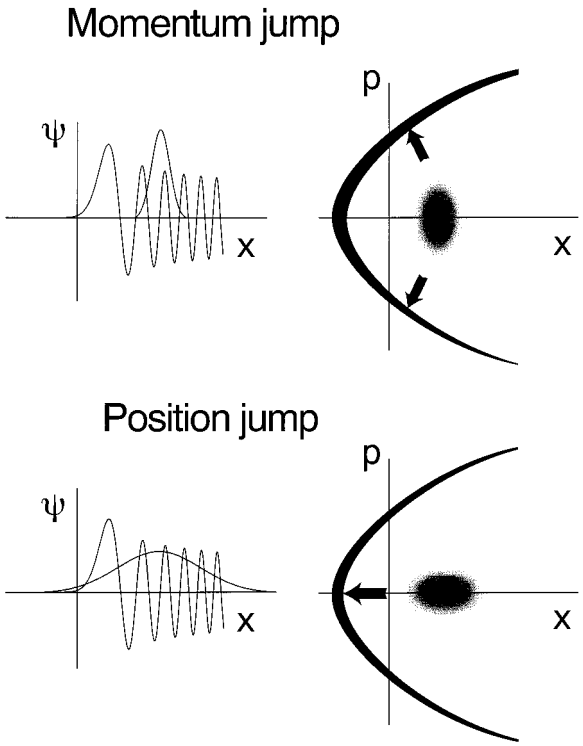

Figure 15. Phase space view giving the Wigner distribution of the initial state and the phase space track of the final state. Depending on the position and momentum uncertainty in the initial state, the tunneling proceeds by position jumping or combination momentum-position jumping.

$$k = \frac{2\pi}{\hbar}\langle V^2\rangle\rho(E_0) \tag{34}$$

where $\rho(E_0)$ is the density of states at energy E_0, and $\langle V^2\rangle$ is the mean-square matrix element. Making the Condon approximation, we write this as

$$k = \frac{2\pi}{\hbar}V_0^2\,\mathrm{Tr}[\delta(E_0 - H_a)|d\rangle\langle d|]$$

$$\equiv \frac{2\pi}{\hbar}V_0^2\,\mathrm{Tr}[\delta(E_0 - H_a)\rho_d] \tag{35}$$

where $|d\rangle$ is the donor wavefunction, V_0^2 is the constant coupling strength, and $\rho_d = |d\rangle\langle d|$ is the density matrix for the donor wave function. We simplify this further here by approximating eq 35 as

$$k \approx \frac{2\pi}{\hbar}V_0^2\int \mathrm{d}\vec{p}\,\mathrm{d}\vec{q}\;\delta[(E_0 - H_a(\vec{p},\vec{q}))]\;\rho_d^W(\vec{p},\vec{q}) \tag{36}$$

The approximate expression 36 gives the rate k as proportional to the integral of the Wigner density of the donor, $\rho_d^W(\vec{p},\vec{q})$, over the classical energy hypersurface $\delta[E_0 - H_a(\vec{p},\vec{q})]$ of the acceptor. We ask: where on the acceptor energy surface does the bulk of the rate integral come from? This is a matter of investigating the *integrand* of eq 36. We are treating the donor and acceptor wavefunctions differently. The donor is given a full fledged Wigner density, the acceptor is treated as a classical energy hypersurface.

By studying the phase space structure of the donor wavefunction and the energy hypersurface of the acceptor Hamiltonian, we learn where amplitude appears on the acceptor potential energy surface. The rate k is proportional to the average Franck−Condon factor; it is a non-state specific quantity. By interpreting the integrand of eq 36, we are putting back the specificity in a very useful way, by saying where (and with what velocity) the amplitude appears on the acceptor surface.

Considered as a Wigner phase space distribution, the donor wavefunction is a smooth distribution peaked at zero momentum. In coordinate space it is peaked at the minimum of the donor potential energy surface. The bulk of such a phase space density *has too low an energy* on the *acceptor* potential energy surface to be germane to the donor → acceptor transition. The transition has to be quasi-degenerate with the energy of the donor state, which is high, due to its stored electronic energy. To find the relevant regions in phase space we must examine those parts of the "tail" of the Wigner density that have sufficient energy on the acceptor potential energy surface. This is the content of eq 36.

We start with a one dimensional system in Figure 15. Two cases are seen corresponding to blue wing absorption (or red wing emission). The wave functions are shown on the left; on the right, the phase space pictures. The Wigner phase space distribution for the donor state is a smeared distribution, and the quasidegenerate contour interval on the acceptor potential energy surface is the parabolic curve. In the top case, the donor wavefunction is narrow, so the oscillations of the acceptor wave function do not completely kill the integral. Furthermore, the tail of the donor wavefunction is very small near the tail of the acceptor wavefunction. There is no doubt that the overlap comes from the region where the donor wavefunction is large. This is a momentum jump case, because the amplitude leaving the donor wavefunction may be thought of as appearing near the maximum of the donor wave function, with considerable momentum on the repulsive acceptor potential. The phase space picture reflects the increased momentum uncertainty and decreased position uncertainty associated with the narrow

coordinate space distribution. Clearly a shift in momentum at (nearly) constant position gives the shortest path between the two distributions.

At the bottom in Figure 15 we see a much wider donor wavefunction, centered as in the previous case. A glance at the wave function plots shows there is now good overlap of the tails, and more nearly complete cancellation of the integral in the oscillatory region. The integral is coming mostly from the region of the tails, and the phase space plot demonstrates that a position jump (again at zero momentum) gives the shortest path between the two states.

We have just seen that position jumps and momentum jumps can compete to be the major contribution to the Franck−Condon integral in the nonclassical regime. In several dimensions, each position and each momentum become competitors. The winning coordinates can be quite surprising. Thus, for nonclassical transitions, the usual Franck−Condon propensity rules can be very misleading. For example, the mode with the largest equilibrium position displacement need not be excited in a nonclassical Franck−Condon transition in the wings.

In several dimensions, each coordinate and its conjugate momentum becomes a candidate for the location of the "leak". Once again we seek the location in phase space on the final potential's energy hypersurface when the Wigner density of the initial state is largest. As the tunneling gets deeper, this place becomes harder to guess from the obvious features of the two potential energy surfaces. For example, if the "donor" surface is displaced mostly in a coordinate x compared to the acceptor surface, we would normally expect the x-coordinate to be involved in the leaky region. Indeed this will be the case for not too deep tunneling, as happens if the distance between the surfaces is not too great. However, as the tunneling gets deeper, other effects tend to dominate, such as the size and differences in force constants on the two surfaces.

An important and illustrative example which is well understood from the usual Franck-Condon perspective involves two surfaces with a moderate displacement in a moderate frequency normal mode a together with a small displacement in a high frequency mode b. The Franck−Condon factors are (in the separable limit) products of one dimensional Franck-Condon factors; in this case

$$F_{nm} = \langle \bar{0}_a | n_a \rangle \langle \bar{0}_b | m_b \rangle \tag{37}$$

where the requirement of quasi-degeneracy $E_{na} + E_{mb} \approx E_{\bar{0}\bar{0}}$ is enforced. The bar indicates a state on the initial donor potential energy surface. The issue of where the leak is has been addressed before: which term F_{nm} dominates in the average appearing in the Golden rule expression

$$k \propto \frac{2\pi}{\hbar} < F_{nm}^2 > \rho \tag{38}$$

Note that whatever the answer to this question, it is much less specific than our phase space leak formulation, since the winning state $|n_a m_b\rangle$ is itself potentially rather extended in phase space. If there is truth to the notion that a small region of phase space dominates, it would concomittantly imply that other states $|n_a' m_b'\rangle$ would also have to have substantial overlap.

Figure 16 illustrates the tunneling question for two displaced Born−Oppenheimer surfaces. Will the wavefunction leal onto the lower surface by a position jump, or a momentum jump, or some combination, and in which coordinates?

Reference 35 was concerned mainly with radiationless rates as a function of excess vibrational energy, in the tunneling regime. An intriguing aspect of this work was that the departure points for the tunneling paths in position space were the corner caustics, in the case that the motion was integrable on the initial surface. Here, we focus with the overlaps as a function of electronic energy (or the "energy gap"), as well as other features of the participating Born−Oppenheimer potential energy surfaces. The earlier work considered only what we shall refer to here as position jump (as opposed to momentum jump) nonclassical transitions.

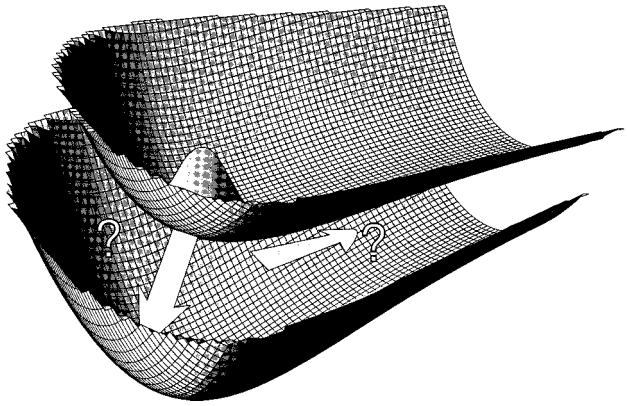

Figure 16. Matters get really interesting when for nested potential energy surfaces in several dimensions a competition is set up to determine which position or momentum coordinate, or combination coordinate, is the location of the "leak" between the two surfaces.

V. Dissociative Tunneling of a van der Waals Cluster

A final example raises an interesting question: can we treat some systems by either approach, i.e. two surface Born−Oppenheimer or resonance zone induced dynamical tunneling? Clearly, there is a common element, which deserves more attention than we can give it here: the idea of slowness of one or more coordinates. In Born−Oppenheimer, it is the essence of the approach, and in the resonance analysis, one goes over to a slow angle, which might be viewed alternately as an adiabatic coordinate. Are the two approaches really the same? Certainly not in the details.

In a van der Waals complex undergoing vibrational predissociation, one could treat the fast vibration as the "electronic" degree of freedom, and the van der Waals bond (usually much lower frequency) as the slow coordinate. So the Born−Oppenheimer approximation applies. On the other hand, a classical resonance analysis also would apply, based on action-angle variables as outlined above.

Finally, there is a third alternative, one we have been avoiding so far: perturbation theory based on an uncoupled H_0. This was Ewing's perspective,[30] and it is qualitatively very successful. The generalization outlined in this paper shows that there is no need to be in the perturbative regime, for the weak tunneling interactions we have been discussing to apply. This would allow a classical trajectory analysis on a fully coupled potential energy surface followed by identification of resonance islands, with a final perturbation expression based not on uncoupled degrees of freedom but rather on the full action angle variables for the system.

VI. Conclusion

We have concentrated on dynamical tunneling in the first part of this paper, and on Born-Oppenheimer surface-to-surface tunneling in the second part. Many of our examples are not

traditionally conceived of in terms of tunneling, but are usefully and properly understood this way.

Dynamical tunneling, we conjecture, may often be the mysterious agent of IVR which experimentalists speak about. Over the years, we have found that a useful definition of IVR is whatever experimentalists do not understand or cannot assign, leading to decay, fractionation of spectra, etc. Thus, when certain spectral features are explained theoretically in terms specific mode-to-mode coupling, occurring resonantly and in an orderly way, this is *not* considered to be IVR, much to the consternation of the theorist! But experimentalists have good reason for this. IVR is a rolling concept: we can define zero order states which involve a limited number of degrees of freedom and which incorporate all the above mentioned resonant coupling. These zero order states now may decay on a much longer time scale, and for less well understood reasons, leading to fractionated spectra with total bandwidths as small as 0.01 cm^{-1}. This is IVR, and we suggest it may be due to dynamical tunneling.[5,7]

Born−Oppenheimer surface-to-surface tunneling is the main actor in a large sector of chemistry and chemical physics. Much of the time, surface-to-surface amplitude transfer is classically allowed, perhaps through thermal activation. This situation yields to surface hopping approximations at the classically allowed surface intersections, and is much better understood and classified.[36]

Photochemistry, especially on the regime of high quantum yield (slow radiationless decay), photoabsorption and photoemission in the far wings of spectroscopic bands, vibrational predissociation, and nonresonant electron transfer are important examples of the tunneling regime of Born-Oppenheimer potential energy surface coupling. Just as the study of molecular vibrations and rotations has extended beyond the realm of normal modes and assignable spectra to nonlinear dynamics and even chaos, so too should the study of intersystem crossing, internal conversion, electron transfer, etc., embrace modern dynamical concepts

Acknowledgment. From an early stage in my research until the present time, Kent Wilson has enlightened, inspired, guided and encouraged me with his patented enthusiasm and unique intellect. Discussions over the years with Kent have shaped my scientific life, including the work reported here. I am greatly indebted to him. This research was supported by the National Science Foundation under grant CHE-9610501, and through ITAMP at the Harvard-Smithsonian Center for Astrophysics.

References and Notes

(1) Reimers, J. R.; Wilson, K. R.; Heller, E. J. *J. Chem. Phys.* **1983**, *79*, 4749.

(2) Reimers, J. R.; Wilson, K. R.; Heller, E. J.; Langhoff, S. R. *J. Chem. Phys.* **1985**, *82*, 5064.

(3) Gordon, R. G. *Adv. Magn. Reson.* **1968**, *3*, 1. Berens, P. H.; Wilson, K. R. *J. Chem. Phys.* **1981**, *74*, 4872. Heller, E. J. *Acc. Chem. Res.* **1981**, *14*, 368.

(4) Heller, E. J.; Stechel, E. B.; Davis, M. J. *J. Chem. Phys.* **1980**, *73*, 4720−35.

(5) Heller, E. J.; Davis, M. J. *J. Phys. Chem.* **1981**, *85*, 307−09.

(6) Lawton, R. T.; Child, M. S. *Mol. Phys.* **1979**, *37*, 1799; *Mol. Phys.* **1981**, *44*, 709.

(7) Heller, E. J. *J. Phys. Chem.* **1995**, *99*, 2625.

(8) Harter, W. G.; Patterson, C. W. *J. Chem. Phys.* **1984**, *80*, 4241.

(9) Maitra, N. T.; Heller, E. J. *Phys. Rev. A* **1997**, *54*, 4763.

(10) Landau, L. D.; Lifshitz, E. M. *Quantum Mechanics (Non-relativistic Theory)*; Pergamon Press: New York, 1977.

(11) Davis, M. J.; Heller, E. J. *J. Chem. Phys.* **1981**, *75*, 246−54.

(12) Maitra, N.; Heller, E. J. *Phys. Rev. Lett.* **1997**, *78*, 3035.

(13) Miller, W. H. *Adv. Chem. Phys.* **1974**, *25*, 69.

(14) Keshavamurthy, S.; Miller, W. H. *Chem. Phys. Lett.* **1994**, *218*, 189.

(15) Farrelly, D.; Uzer, T. *J. Chem. Phys.* **1986**, *85*, 308.

(16) Ozorio de Almeida, A. M. *J. Phys. Chem.* **1984**, *88*, 6139.

(17) Roberts, F. L.; Jaffe, C. *J. Chem. Phys.* **1993**, *99*, 2495.

(18) Ramachandran, B.; Kay, K. *J. Chem. Phys.* **1993**, *99*, 3659.

(19) Miller, W. H. *J. Chem. Phys.* **1970**, *53*, 1949, 3578.

(20) Faltermeier, B.; Protz, R.; Maier, M. *Chem. Phys.* **1981**, *62*, 377.

(21) Skinner J. Private communication.

(22) Davis, M. J.; Heller, E. J. *J. Phys. Chem.* **1981**, *75*, 246.

(23) Stechel, E. B.; Heller, E. J. *Ann. Rev. Phys. Chem.* **1984**, *35*, 563−589. Heller, E. J.; Sundberg, R. L. In *Chaotic Behavior in Quantum Systems*; Casati, Giulio, Ed.; Proceedings of a NATO Advanced Research Workshop on Quantum Chaos; Plenum Publishing Corporation, 1985. Heller, E. J. *Phys. Rev. Lett.* **1987**, *A35*, 1360.

(24) Lehmann, K. K.; Pate, B. H.; Scoles, G. *Ann. Rev. Phys. Chem.* **1994**, *45*, 241. Kerstel, E. R. Th.; Lehmann, K. K.; Mentel, T. F.; Pate, B. H.; Scoles, G. *J. Phys. Chem.* **1991**, *95*, 8282.

(25) Minton, T. K.; Kim, H. L.; Reid, S. A.; McDonald, J. D. *J. Phys. Chem.* **1988**, *89*, 6550.

(26) McIIroy, A.; Nesbitt, D. J. *J. Chem. Phys.* **1989**, *91*, 104; *J. Chem. Phys.* **1990**, *92*, 2229.

(27) Stechel, E. B.; Heller, E. J. *Ann. Rev. Phys. Chem.* **1984**, *35*, 563−589. Heller, E. J.; Sundberg, R. L. In *Chaotic Behavior in Quantum Systems*; Casati, Giulio, Ed.; Proceeding of a NATO Advanced Research Workshop on Quantum Chaos; Plenum Publishing Corporation; 1985. Heller, E. J. *Phys. Rev. Lett.* **1987**, *A35*, 1360.

(28) Heller, E. J. Wave packet dynamics and quantum chaology. In *Lectures in the 1989 NATO Les Houches. Summer School on Chaos and Quantum Physics*; Giannoni, M-J., Voros, A., Zinn-Justin, J., Eds.; Elsevier Science Publishers B.V.: Amsterdam, 1991; p 547. Heller, E. J. *J. Chem. Phys.* **1977**, *67*, 3339−51.

(29) Heller, E. J.; Beck, D. *Chem. Phys. Lett.* **1993**, *202*, 350.

(30) Ewing, G. E. *J. Chem. Phys.* **1979**, *71*, 3143−3144.

(31) Nikitin, E. E.; Noda, C.; Zare, R. N. *J. Chem. Phys*. **1993**, *98*, 46−59.

(32) Medvedev, E. S. *Chem. Phys.* **1982**, *73*, 243−251.

(33) Heller, E. J. Spectroscopy and dynamics in the wings. In *Molecular Dynamics and Spectroscopy by Stimulated Emission Pumping*; Dai, Hai-Lung, Field, R., Eds.; World Scientific: River Edge, NJ, 1995.

(34) Segev, B.; Heller, E. J. *J. Chem. Phys.* **1999**. In press.

(35) Heller, E. J.; Brown, R. C. *J. Chem. Phys.* **1983**, *79*, 3336.

(36) See Sholl, D. S.; Tully, J. C. *J. Chem. Phys.* **1998**, *109*, 7702 and references therein.

(37) However, sometimes a canonical transformation can give a new Hamiltonian with a barrier in the new variables where none existed in the original coordinates.